Subharmonically Pumped Millimeter-Wave Mixers

ERIC R. CARLSON, MEMBER, IEEE, MARTIN V. SCHNEIDER, FELLOW, IEEE, AND THOMAS F. McMASTER, MEMBER, IEEE

Invited Paper

Abstract—**The two-diode subharmonically pumped stripline mixer has a pair of diodes shunt mounted with opposite polarities in a stripline circuit between the signal and local oscillator inputs. The circuit has low noise and conversion loss and substantial AM local oscillator noise cancellation. The local oscillator frequency is about half the signal frequency. A novel diode chip, the notch-front diode, which has ohmic contacts on the chip faces adjacent the face containing the diode junctions, was developed for these circuits. The notch-front diode permits the low parasitic reactance of the waveguide diode mount to be achieved in stripline circuits. The best performance for a two-diode subharmonically pumped mixer with notch-front diodes was a 400 K mixer noise temperature, obtained at 98 GHz, which is comparable to the best fundamental mixers in this frequency range. The performance over a 47–110-GHz frequency range for this circuit with commercial beam-lead diodes is also presented.**

I. INTRODUCTION

THE TWO-DIODE subharmonically pumped hybrid integrated downconverter [1], [2], referred to here as the two-diode mixer, has many desirable properties which make it an interesting alternative to conventional mixers, especially at millimeter wavelengths. The local oscillator requirements are easier to meet in a two-diode mixer because the LO frequency is about half that in the corresponding conventional mixer, and because the two-diode mixer has substantial AM local oscillator noise suppression [3]. The large difference between the signal and LO frequencies simplifies the design of a filter to separate these frequencies and permits elimination of the potentially lossy diplexing arrangement used at the signal input of conventional mixers. The position of this stripline filter can be readily changed to optimize the impedance seen by the diode looking toward the local oscillator port. The two-diode mixer described here can be tuned for either single-sideband or double-sideband response, and covers an entire waveguide band. Due to the symmetry of the circuit, the diode-pair current contains no even harmonics of the LO [4], so that no dc return path is needed, and emission from the mixer in the signal frequency band is suppressed. Passive elements are incorporated in the strip transmission line circuit with high precision by conventional photolithographic techniques rather than by intricate machining. And, as discussed below, the noise and loss performance of the two-diode mixer is comparable to the best fundamental mixers.

When compared with second-harmonic mixers employing a single diode [5], [6], the two-diode mixer has another important advantage. The conductance waveform of the diode pair contains only even harmonics of the LO [4], so the two-diode mixer is inherently insensitive to frequencies in the band corresponding to fundamental mixing with the local oscillator. Response at these frequencies must be suppressed by the embedding network of the single-diode second-harmonic mixer, and a nonreactive termination will result in a contribution to the mixer noise. Furthermore, in practice, in single-diode second-harmonic mixers, a filter structure to separate the signal and LO frequencies has not been used, so that the impedance at the signal frequency seen by the diode looking toward the LO port has not been optimized.

A novel diode chip geometry, which we call the notch-front diode [7], was developed for use in strip transmission line circuits. This chip has ohmic contact metallization on the chip faces adjacent to the face containing the diode junctions. Notch-front diodes can be readily soldered to millimeter-wave thin-film circuits. They are particularly suited for use in conventional and subharmonically pumped millimeter-wave mixers because the reduced parasitic capacitance in comparison with beam-lead diodes results in a better switching waveform and because the chip geometry has a lower RF series resistance than conventional millimeter-wave diode structures.

Results have been obtained over a 66–110-GHz frequency range for notch-front and beam-lead diodes in the two-diode downconverter. The best performance with notch-front diodes, a single-sideband (SSB) mixer noise temperature of 400 K at 98 GHz, is comparable to the best results of fundamental mixers in this frequency range. In comparison, beam-lead diodes in this mixer at 98 GHz had a SSB mixer noise temperature of 1600 K and required 10 dB more local oscillator power. At lower frequencies, the performance of the beam-lead diode mixer improves as parasitic effects become less important.

These two-diode downconverters look promising for scaling to other frequencies. Potential applications include

Manuscript received November 3, 1977.

E. R. Carlson and M. V. Schneider are with Bell Laboratories, Crawford Hill Laboratory, Holmdel, NJ 07733.

T. F. McMaster is with Bell Laboratories, Holmdel, NJ 07733.

0018-9480/78/1000-0706$00.75 ©1978 IEEE

microwave and millimeter-wave communications, plasma diagnostics, collision avoidance radar, and radio astronomy.

This paper mainly discusses results in the 66–110-GHz frequency range for two-diode mixers with a WR-10 input waveguide. Preliminary reports of these results have appeared [4], [8]. The design and performance of two-diode mixers at 5 GHz and 50 GHz have also been published [4] and are briefly reviewed here.

II. Circuit Description

Stripline, i.e., suspended-substrate strip transmission line, was used in the design of this mixer because it has lower loss and less excitation of higher modes than conventional microstrip. The mixer circuit was optimized in a large scale model at a signal frequency of about 5 GHz, and then all circuit dimensions were reduced by the ratio of the model and millimeter-wave signal frequencies to make the millimeter-wave mixers [4].

A schematic view of the stripline conductor pattern is shown in Fig. 1, and a photograph of the millimeter-wave mixer with the cover removed is presented in Fig. 2. The circuit consists of a signal waveguide input section, a waveguide to stripline transition, a stripline conductor pattern including mounting pads for a pair of Schottky barrier diodes and two low-pass filters, and a transition from the LO waveguide to the stripline. The signal waveguide to stripline transition, illustrated in Fig. 3, can be tuned by adjusting the waveguide backshort and the *H*-plane waveguide short so that the downconverter can be operated either as a single-sideband or as a double-sideband mixer.

The input signal is coupled to a pair of Schottky barrier diodes which are shunt mounted on the stripline with opposite polarities. The notch-front diodes were soldered to the stripline conductor. The commercial beam-lead diodes [9] were thermocompression bonded to the circuit.

Two low-pass filters are needed to separate the signal frequency $\omega_s = 2\omega_p \pm \omega_{IF}$, the LO frequency ω_p and the intermediate frequency ω_{IF}. The filter adjacent to the pair of diodes has a cutoff frequency of 59 GHz in order to reject the signal (66–110 GHz) while transmitting the LO (32.3–54.3 GHz) and the IF (1.4 GHz). In the lumped-element approximation, it is a seven-element *L*–*C* ladder type low-pass filter with a Chebyscheff response. The second low-pass filter was designed empirically to reject the LO frequency and transmit the IF.

The stripline conductor pattern is fabricated using standard thin-film and photolithographic techniques. The substrates are polished optical-grade fused quartz 0.12 mm thick. The conductor metallization, deposited by evaporation, is 2.0–2.5 μm of gold on top of 75–150 Å of chromium. The surface finish of the metallization was found to be important: mixers made on substrates with matte finish metallization had conversion losses almost one dB higher and mixer noise temperatures several hundred degrees higher than mixers made on substrates with mirror finish metallization.

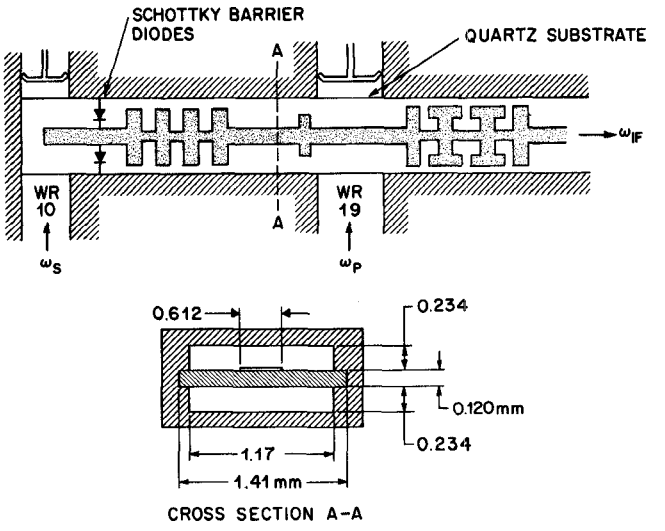

Fig. 1. Top view and cross-sectional view of the stripline circuit with signal and LO waveguide input ports. The LO waveguide was WR-15 for the first version of the circuit, including mixer 113.

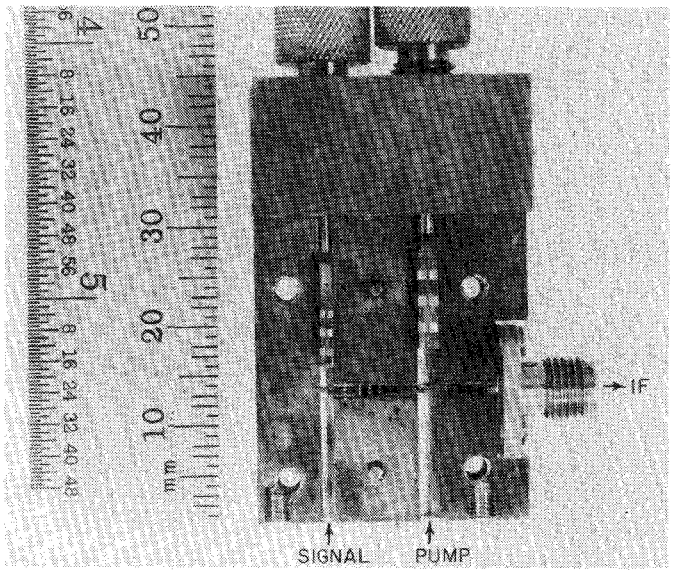

Fig. 2. Photograph of the low noise mixer. The top cover of the housing is removed to show the conductor pattern on the quartz substrate and the mounted diodes.

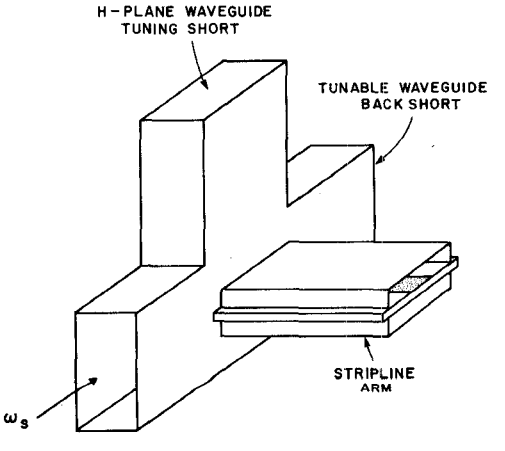

Fig. 3. Transition from signal waveguide to stripline circuit with a tunable waveguide backshort and an *H*-plane tunable short.

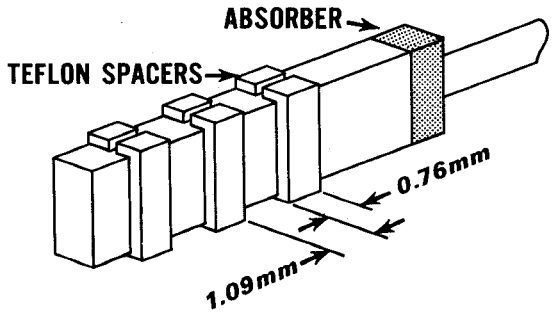

Fig. 4. Sliding noncontacting waveguide short used in these mixers. The dimensions shown are for WR-10 waveguide in which the narrow sections are 0.20 mm wide and the wide sections are 1.19 mm.

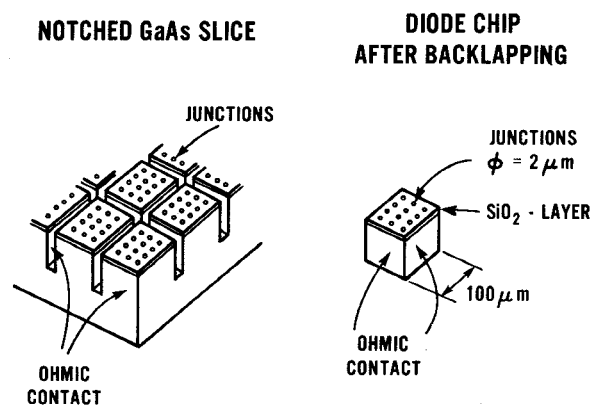

Fig. 5. Schematic view of notched GaAs slice and diode chip after backlapping.

The circuit housing was machined from OFHC copper. The first housing had a WR-15 local oscillator waveguide scaled from the low-frequency model, and the cutoff of this waveguide placed a lower limit of about 85 GHz on the circuit operation. Subsequently it was found that the LO waveguide could be changed to WR-19 and circuit operation extended below 70 GHz without any penalty in performance at higher frequencies.

The sliding noncontacting shorts used in both the signal and LO waveguides had alternating high and low impedance sections as shown in Fig. 4. The shorts were smooth and stable in operation and across the waveguide band had a reflection coefficient greater than or equal that of a solid copper plate terminating the waveguide.

III. Notch-Front Diodes

A novel diode chip geometry was developed which has low parasitics and can readily be mounted in strip transmission line circuits. This structure, called the notch-front diode [7], has ohmic contacts and an array of junctions fabricated on adjacent sides of a chip as shown in Fig. 5. A silicon dioxide layer with a thickness of 5000 Å is first deposited on the epitaxial layer side of a gallium arsenide slice. An array of notches is cut into the GaAs slice with a diamond saw blade. The slice has a thickness of approximately 300 μm and the notches are cut to a depth of 100 μm. An ohmic contact is formed in the notches by electroplating Sn–Ni, Ni, and Au into the notches and subsequently alloying the slice at a temparature of 400°C for 60 s. The ohmic contact metallization is about 1 μm thick. The notches are filled with photoresist and an array of Schottky barrier diodes is fabricated on the front of the slice by a sequence of processing steps involving masking with photoresist, plasma etching of holes into the SiO_2 layer which covers the top surface of the slice, and electroplating of platinum and gold on the exposed GaAs surface in the hole areas. A pulse plating technique developed by Burrus [10] is used to obtain uniform deposition of the metal films in all the hole areas. A description of the junction formation steps is given in a separate paper [11].

N-type vapor phase epitaxy material was used in this work. The epitaxial layer was about 1200 Å thick and was doped with sulphur to a carrier concentration of about 2×10^{17} cm^{-3}. The dopants for the buffer layer and substrate were sulphur and silicon, respectively, and the carrier concentration was about 3×10^{18} cm^{-3}.

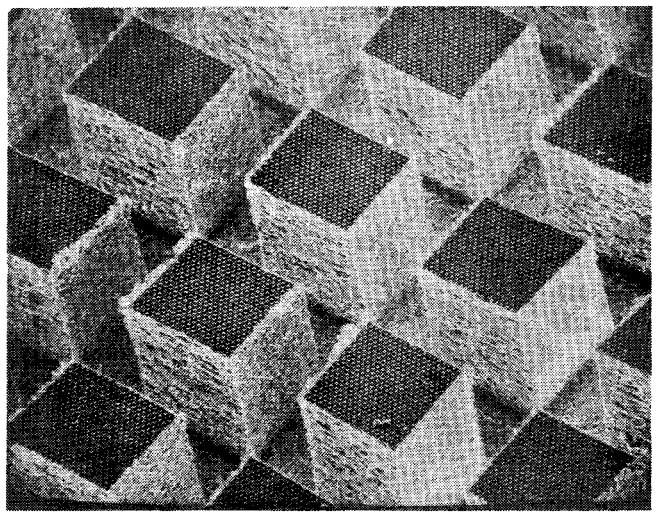

Fig. 6. Scanning electron micrograph of notch-front diodes with a dice size of 75 μm$\times$80 μm and a notch depth of 100 μm. The junction diameter is 2 μm with a center-to-center spacing of 5 μm.

Fig. 6 is a scanning electron micrograph of the slice after fabricating the notches with ohmic contacts and the junctions on top of the slice. The width of the notches is about 70 μm. While some overplating of gold is visible around some parts of the top periphery of each chip, this overplating does not affect the performance of the final device. The individual junctions on the top surface of the slice have a diameter of 2 μm and a center-to-center spacing of 5 μm. With this array of junctions, a diode may be contacted anywhere on the surface of the chip [12]. Individual diode chips are fabricated by mounting the notched slice on a glass slide with wax with the top surface down and backlapping the slice to a thickness which is smaller than the depth of the notches. The chips are separated by dissolving the wax in a solvent. An individual diode chip after the backlapping of the slice is illustrated in Fig. 5. A typical length of the side of the chip is 75 μm. The minimum length is determined by the depth of the damage created by the diamond saw blade which is about 10 μm.

TABLE I
LOW-FREQUENCY PARAMETERS FOR NOTCH-FRONT DIODES

Batch	R_S (Ω)	C_O (fF)	n	V_B(V)
B20-99	8	7	1.13	9
B20-119	7	8	1.12	8
B17-122A	5	8	1.15	8
Conventional Chips	4	8	1.15	8

Two orthogonal sets of parallel notches are cut in the slice to define the diode chips. Chips with ohmic contacts on all four side faces or on two opposite side faces can be made depending on whether the second set of notches is cut before or after the slice is processed to form the ohmic contacts and the diodes. Both types have been made; better diodes were obtained on chips with ohmic contacts on two side faces due to details of the processing techniques.

Typical parameters for three batches of notch-front diodes are shown in Table I. The series resistance R_s measured at 10-mA forward current, and the n-factor are taken from dc I–V characteristics for chips mounted in circuits, The reverse breakdown voltage V_B and the zero-bias junction capacitance C_0 were measured in unmounted chips. A 1-MHz capacitance bridge was used to measure C_0. The series resistance was reduced as processing technology improved through experience. Also listed in Table I are the parameters for one of our best conventional diodes with the ohmic contact on the back of the chip. The low-frequency parameters for the notch-front diodes are not significantly different from those for the coventional chip. The commercial beam-lead diodes used in these circuits typically had $R_s \approx 3.5$ Ω and a total capacitance of about 60–75 fF.

Although these low-frequency measurements may not be sufficient to predict completely the performance of a mounted device at millimeter wavelengths [13], [14], they are useful as the most widely compared characteristics of Schottky barrier diodes. Sources of the series resistance for a millimeter-wave diode are considered in Appendix A, where it is shown that the series resistance contributed by the skin effect in the notch-front diode is about 2/3 that in a conventional chip. However, the total series resistance in both cases is dominated by effects near the junction.

Notch-front diodes are mounted on the stripline conductor of the millimeter-wave mixers as shown in Fig. 7. The chip is soldered on one side of a gap in the conductor with an indium-based solder [15], and contact is made to a diode on the chip by a pointed spring wire soldered on the other side of the gap with another, lower temperature, indium-based solder [16]. The wire used for the diode contact is 12-μm diameter Phosphor Bronze A. A point is etched on the end of the wire at 1.2-V dc in an electrolyte consisting of 23-ml H_2SO_4, 80-ml H_3PO_4, 1.5-g CrO_3, and 50-ml H_2O [17], with a final dilution of about one part H_2O to ten parts of the above solution to allow for constituent concentration variations. A typical point, shown in Fig. 8, has a tip radius of about 1 μm to contact

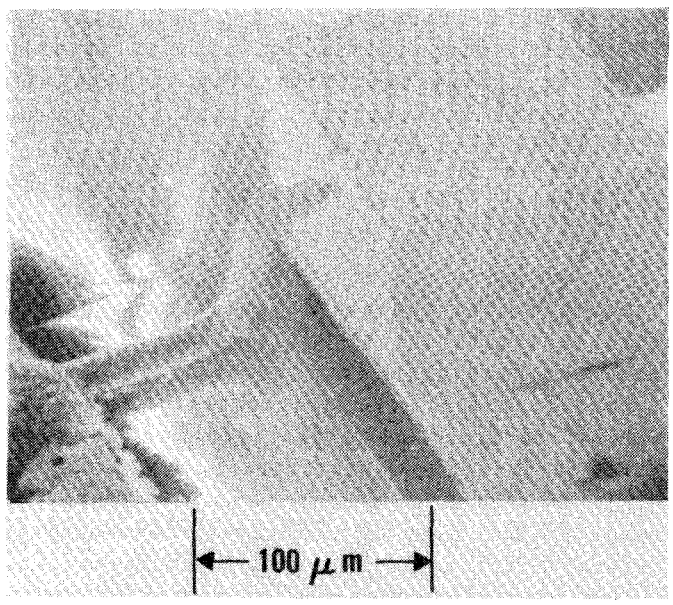

Fig. 8. Scanning electron micrograph of a pointed 12-μm diameter phosphor bronze wire used for making contact to Schottky barrier diodes.

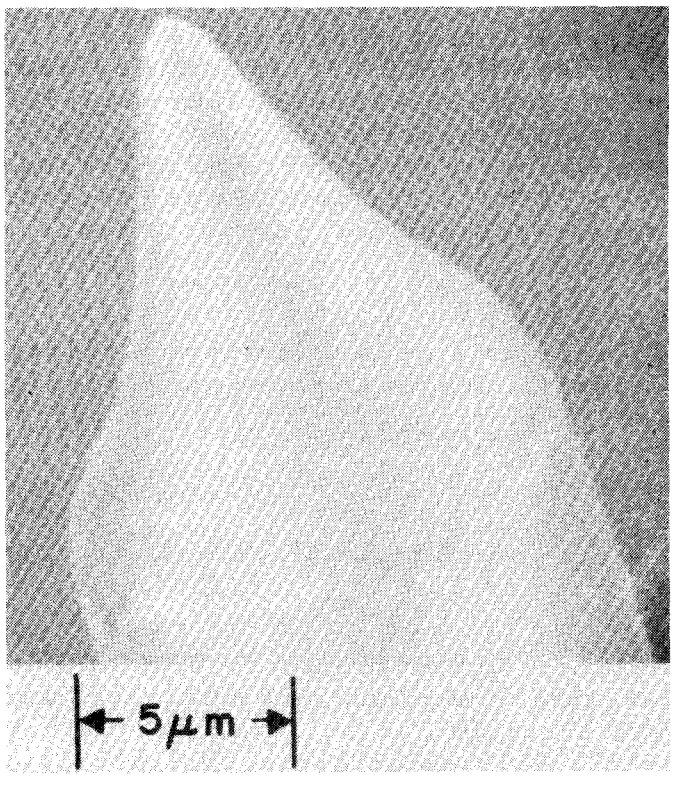

Fig. 8. Scanning electron micrograph of a pointed 12-μm diameter phosphor bronze wire used for making contact to Schottky barrier diodes.

the 2-μm diameter junctions without penetrating to the epilayer, and a large included angle to reduce parasitic inductance and minimize susceptibility to damage during the contacting process. A spring having the shape shown in Fig. 7 is bent with a micromanipulator, and the wire is then stress relieved for one hour at 218°C in a forming gas atmosphere. The two chips are simultaneously soldered to the substrate on a strip heater. The substrate with the

mounted chips is clamped in the mixer block before the diodes are contacted. and the IF port connection is made so that the diode dc characteristics can be monitored during assembly. The assembly is performed with micromanipulators under a stereo microscope.

IV. Measurement Procedure

The performance of the mixers was determined by measuring their response to both noise and coherent input signals. We consider a mixer with responses at only two frequencies, the signal and image, and call this a "dual-response" mixer. In a dual-response mixer the conversion losses for the signal and image L_s and L_i need not be equal. The dual-response mixer includes as special cases the "double-sideband" mixer for which $L_s = L_i$ and the "single-sideband" mixer for which $L_i = \infty$. Mixer noise is expressed in terms of mixer input noise temperature T_M, the temperature of the input termination on an equivalent noise-free mixer which would produce the same output noise power as the actual mixer with a noise-free input termination [18]. Similarly, a receiver input noise temperature T_R can be defined which includes the noise contributed by both the mixer and the IF amplifier.

For a dual-response receiver, the result of a Y-factor measurement [19] using a broad-band noise source is a "dual-sideband" receiver noise temperature T_R (DSB). If the signal of interest appears in the signal sideband only, then the appropriate measure of receiver noise is the single-sideband receiver noise temperature, given by

$$T_R(\text{SSB}) = \left(1 + \frac{L_s}{L_i}\right) T_R(\text{DSB}). \tag{1}$$

A similar equation applies to mixer noise temperature. The mixer and receiver noise temperatures are related by

$$T_R(\text{SSB}) = T_M(\text{SSB}) + L_s T_{\text{IF}} \tag{2a}$$

or by

$$T_R(\text{DSB}) = T_M(\text{DSB}) + \frac{L_s}{1 + \frac{L_s}{L_i}} T_{\text{IF}} \tag{2b}$$

where T_{IF} is the noise temperature of the IF amplifier. Some results are expressed in terms of the receiver noise figure given by [20]

$$F_R(\text{SSB}) = \left(1 + \frac{L_s}{L_i}\right)\left[1 + \frac{T_R(\text{DSB})}{290}\right]. \tag{3}$$

The relationships between single-sideband and dual-sideband noise temperature and noise figure are summarized in Fig. 9.

The noise power at the IF output P_n was measured for three different conditions [18]:

1) mixer terminated with a hot load:

$$P_n(H) = \left[(T_H + T_M)\left(\frac{1}{L_s} + \frac{1}{L_i}\right) + T_{\text{IF}}\right] kBG_{\text{IF}} \tag{4}$$

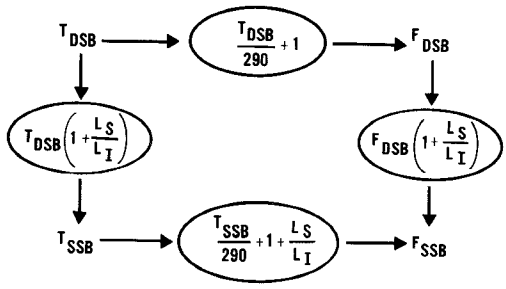

Fig. 9. Noise relationships in dual-response receivers for single-sideband, SSB, and dual-sideband, DSB, noise temperature, T, and noise figure, F, where L_s and L_i are the signal and image conversion losses. The relationships apply to both receiver and mixer noise temperature or noise figure.

2) mixer terminated with a cold load:

$$P_n(C) = \left[(T_C + T_M)\left(\frac{1}{L_s} + \frac{1}{L_i}\right) + T_{\text{IF}}\right] kBG_{\text{IF}} \tag{5}$$

3) IF amplifier terminated with a hot load:

$$P_n(\text{IF}) = [T_H + T_{\text{IF}}] kBG_{\text{IF}} \tag{6}$$

where T_M is the DSB mixer noise temperature, T_H is the temperature of the hot load, T_C is the temperature of the cold load, k is Boltzmann's constant, B is the bandwidth, and G_{IF} is the IF gain. The mixer termination was a piece of millimeter-wave absorber at room temperature, $T_H =$ 299 K, or soaked with liquid nitrogen, $T_C = 77$ K. The IF amplifier termination was a coaxial load at room temperature. The IF noise temperature was measured separately with hot and cold loads [21]. Transistor amplifiers with $T_{\text{IF}} = 330$ K and $T_{\text{IF}} = 438$ K and an uncooled paramp for which $T_{\text{IF}} = 108$ K were used in the 1.4-GHz IF system. The IF output power was measured with a thermocouple power meter [22] coupled to a digital voltmeter for increased resolution. The Y factors $Y_H = P_n(H)/P_n(\text{IF})$ and $Y_C = P_n(C)/P_n(\text{IF})$ can be solved for the signal conversion loss:

$$L_s = \frac{T_H - T_C}{(Y_H - Y_C)(T_H + T_{\text{IF}})}\left(1 + \frac{L_s}{L_i}\right) \tag{7}$$

and the SSB mixer noise temperature:

$$T_M(\text{SSB}) = L_s[T_H Y_H + T_{\text{IF}}(Y_H - 1)] - T_H\left(1 + \frac{L_s}{L_i}\right). \tag{8}$$

These solutions are indicated graphically in Fig. 10.

Coherent power measurements of L_s and L_i were made to obtain the image rejection ratio L_s/L_i needed to evaluate (7) and (8). The millimeter-wave signal generator shown in Fig. 11 was used to inject into the mixer a known amount of power at the signal or image frequency. The conversion loss was derived from the ratio of the RF input power and the IF output power measured on the thermocouple power meter. Although the accuracy of the image rejection ratio measurement depends primarily on the frequency response of the thermistor head, the entire system was carefully calibrated so that a comparison of the direct measurement of L_s and the noise power

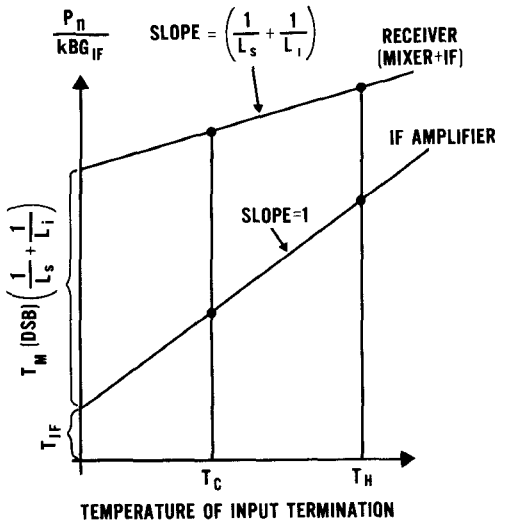

Fig. 10. Noise temperature, referred to the IF amplifier input, as a function of input termination temperature for a receiver and the incorporated IF amplifier. Noise temperature measurements at termination temperatures T_H and T_C are used to obtain the conversion loss and receiver and mixer noise temperatures.

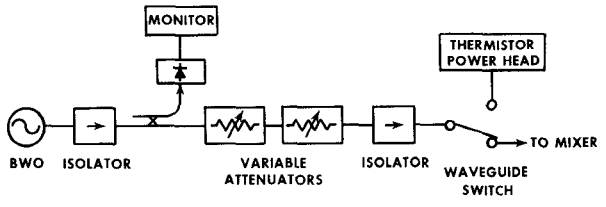

Fig. 11. Block diagram of the millimeter-wave signal generator system used in coherent signal conversion loss measurements.

measurement might serve as an accuracy check. The thermistor head was calibrated across the frequency band against a dry calorimeter [23]. The attenuator linearity was checked with the calorimeter and against the mixer linearity. The IF gain was measured using a set of precision attenuators. The measurement accuracy of the direct conversion loss is estimated to be ± 0.5 dB and of the image rejection ratio to be ± 0.3 dB.

A "simple procedure" (as opposed to the "full procedure" described above) was used to measure some of the data. The receiver noise temperature was determined from the Y factor $Y = P_n(H)/P_n(C)$. The conversion loss and image rejection ratio were obtained from coherent signal measurements, and T_M was calculated from (2). In both cases, the signal generator was used in the initial tuning of the mixer to obtain minimum L_s and the desired L_s/L_i, and a noise tube was then used in the final tuning for minimum F_R before measurement.

For some mixer tunings with large image rejection ratios, it was found that the conversion loss of (7) was about one dB lower then L_s measured directly. Measurement of F_R (SSB) with the signal generator by means of the small-signal method [24] and noise response measurements ((4) and (5)) made with a 2.5-cm length of WR-4 waveguide on the mixer input indicated that the discrepancy was caused by mixer response at higher harmonics. Such data were rejected.

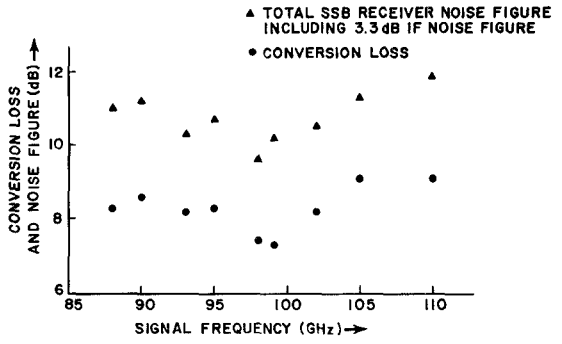

Fig. 12. Total SSB receiver noise figure, including the contribution from a 3.3-dB IF noise figure, and conversion loss of mixer 113 with notch-front diodes as a function of frequency from 85 to 110 GHz. The data points are obtained with the circuit adjusted for optimum receiver noise figure at each frequency. Typical error bars are estimated to be ± 0.2 dB for receiver noise figure and ± 0.5 dB for conversion loss.

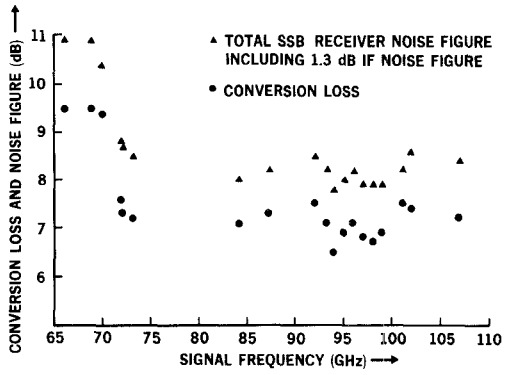

Fig. 13. Total SSB receiver noise figure, including the contribution from a 1.3-dB IF noise figure, and conversion loss of mixer 225 with notch-front diodes as a function of frequency from 66 to 110 GHz. Typical error bars are estimated to be ± 0.1 dB for receiver noise figure and ± 0.2 dB for conversion loss. The circuit was adjusted for minimum receiver noise figure at each frequency.

V. Results

The receiver noise figure and conversion loss for two mixers with notch-front diodes, labeled 113 and 225, are presented in Figs. 12 and 13 and for a mixer with commercial beam-lead diodes labelled TM58 in Fig. 14. Mixer noise temperatures for mixers 113 and 225 and for another mixer with notch-front diodes, labelled 223, are shown in Fig. 15.

The lowest mixer noise temperature measured in a room temperature two-diode mixer was obtained in mixer 113. The comparison of mixers 223 and 225 in Fig. 15 shows the reproducibility obtained with diodes from a slice which has demonstrated uniform properties and substrates from the same batch. The data were taken with the mixer tuned for minimum receiver noise figure at each frequency.

Mixers 223 and 225 were measured by the "full procedure" described in Section IV, and mixer 113 and the beam-lead diode mixer by the "simple procedure." The typical error bars listed are evaluated from the expressions in Appendix B. Mixers 223 and 225 have lower error bars for T_M principally because the IF amplifier used with these mixers had a much lower noise temperature.

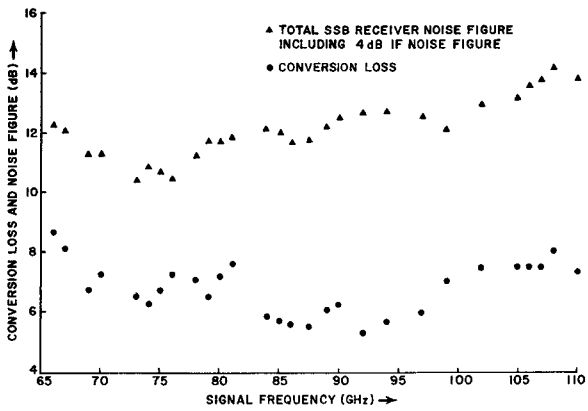

Fig. 14. Total SSB receiver noise figure, including the contribution from a 4-dB IF noise figure, and conversion loss of a two-diode mixer TM58 using commercial beam-lead diodes as a function of frequency. The data points are obtained with the circuit adjusted for optimum receiver noise figure at each frequency. Typical error bars are estimated to be ±0.2 dB for receiver noise figure and ±0.5 dB for conversion loss.

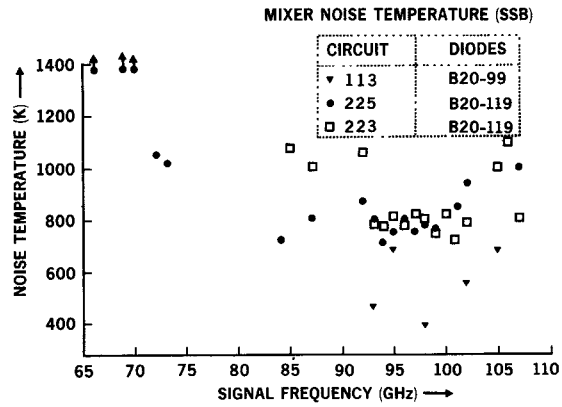

Fig. 15. Mixer noise temperature as a function of frequency of three mixers with notch-front diodes. Typical error bars are ±250 K for mixer 113 and ±60 K for mixers 223 and 225.

Corrections for input loss, LO noise, and IF mismatch are not subtracted from the mixer noise temperature because these effects are unavoidable in making a mixer. The input loss is small because no diplexing arrangement is needed for LO injection as in a conventional mixer. Loss in the input waveguide is estimated to be ~0.1 dB and the corresponding contribution to the mixer noise temperature $\lesssim$25 K. Significant LO noise cancellation occurs in the two-diode mixer [3]. The IF impedance of these two-diode mixers is close to 50 Ω, with return losses greater than 15 dB being measured at the IF port. A tuner between the mixer and IF amplifier eliminated this small mismatch. These corrections are sometimes found to be necessary in characterizing other mixers.

The data are summarized in Table II which includes the lowest mixer noise temperature obtained in each of the three notch-front diode mixers and the lowest noise temperature in the beam-lead diode mixers at both the low end of the signal frequency band (Fig. 14) and the high end [4, Fig. 11]. For comparison, the published performance of several conventional mixers is presented in Table III. For two of these conventional mixers, the data reported [25], [27] includes corrections for IF mismatch. The most important conclusion from these results is that the noise performance of the two-diode mixer with notch-front diodes is comparable to that of the best conventional mixers. Furthermore, the beam-lead diodes can produce competitive results at lower frequencies, although their performance does deteriorate substantially above 85–90 GHz due to device parasitics.

TABLE II
SUMMARY OF RESULTS IN TWO-DIODE MIXERS, 67–110 GHz

MIXER	DIODES	f (GHz)	F_R(SSB)	L_s (dB)	L_i/L_s (dB)	T_M(K)	P_{LO}(dBm)
113	B20-99	98	9.6	7.4	2.9	390±250	+8
223	B20-119	101	7.7	6.5	1.4	720±60	-
225	B20-119	94	7.8	6.5	0.7	710±60	-
TM28	BEAM-LEAD	98	11.3	7.7	4.0	1600±600	+18
TM58	BEAM-LEAD	76	10.4	7.2	2.3	590±310	-

TABLE III
CONVERSION LOSS AND MIXER NOISE TEMPERATURE IN CONVENTIONAL ROOM TEMPERATURE MIXERS AT 70–115 GHz

REFERENCE	f(GHz)	L_s(dB)	T_M(K)
Kerr [25]	85	4.6	420
	115	5.5	500
Wilson [26]	90	5.4	600
	115	6.2	700
Zimmermann &	107	6.2	600
Haas [27]	112	6.1	760
Linke [28]	72	6.2	700
	117	6.5	840

The noise temperature and conversion loss of a resistive mixer are theoretically related by the expression [29], [30]

$$T_M = \frac{nT_p}{2}\left[L_s - 1 - L_s/L_i\right] \tag{9}$$

where T_p is the physical temperature of the diode(s) and where it is assumed that the diode has no series resistance or time-varying junction capacitance. Observed noise temperatures greater than the values given by (9) have been attributed to noise contributions from diode series resistance and the "parametric" effect of the time-varying diode capacitance acting on the correlated components of the diode shot noise [13], [31]. The noise temperature in Table II for mixer 113 is less than, although still consistent with, the theoretical value $T_M = 650$ K predicted by (9). Noise temperatures less than the theoretical value have also been observed in lower frequency two-diode mixers. Two sources could produce such a result, an uncorrected higher harmonic response of the mixer or parametric effects. Although no check for higher

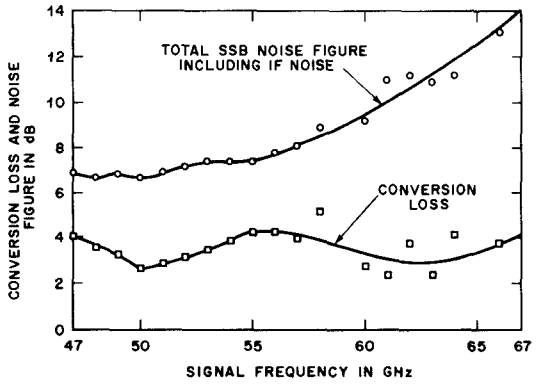

Fig. 16. Total SSB receiver noise figure, including the contribution from a 3.7-dB IF noise figure, and conversion loss of a two-diode mixer using commercial beam-lead diodes as a function of frequency from 47 to 66 GHz. Typical error bars are estimated to be ±0.3 dB for both receiver noise figure and conversion loss.

TABLE IV
PERFORMANCE OF COOLED TWO-DIODE MIXER AT 98 GHz

PHYSICAL TEMPERATURE	L_s(dB)	T_M(K) (SSB)
T=299K	6.8	890
T≈77K	7.0	540

harmonic responses was made with mixer 113, these responses were not observed in other mixers with the type of tuning for which this data was taken. Parametric effects have been seen in two-diode mixers with beam-lead diodes at lower frequencies in the form of conversion gain and also in millimeter-wave fundamental mixers [13]. The operation of a mixer with both variable resistance and variable capacitance has not been fully analyzed, but the general formulation of the problem [31] appears to permit values of T_M either smaller than or larger than that given by (9) for the purely resistive mixer.

The bandwidth of a two-diode mixer with notch-front diodes was measured with the LO frequency and the tuning adjustments fixed. A variation of 0.3 dB in the coherent signal L_S was observed over a 650-MHz frequency band centered at 98 GHz. The instantaneous bandwidth was ultimately limited by the IF amplifier rather than the mixer.

A notch-front diode mixer was cooled to a temperature approaching 77 K by bolting it to a copper bar immersed in liquid nitrogen. The mixer was successfully cooled and returned to room temperature ten times to test the stability of the diodes against thermal stress. The performance of the cooled mixer is given in Table IV and is similar to the results seen in conventional mixers [11], [25].

In Fig. 16 the receiver noise figure and conversion loss for a 47–66-GHz two-diode mixer with beam-lead diodes are reproduced [4, Fig. 9]. In these measurements of F_R, a waveguide noise tube [32] calibrated by the National Bureau of Standards was used. Two points, chosen to represent the low and high end of the frequency band, are

TABLE V
MIXER PERFORMANCE IN 30–70-GHz FREQUENCY RANGE

Reference	f (GHz)	F_R(dB) SSB	L_s(dB)	T_M(K) or F_m(dB) SSB
Two-diode mixer	49	6.9	3.3	290±140 K 3.1±1.0 dB
	60	9.2	2.8	1360±190 K 7.6±0.5 dB
Weinreb and Kerr [33]	33	-	5.9	623 K
Calviello, et al. [34,35]	35	5.9	3.3	3.9 dB
Akaike, et al. [36]	50	10.1	5.3	-
Cohn, et al [2]	55	-	8	-
Meier [35,37]	60	9.0	-	-

listed in Table V. Mixer noise temperature deteriorates at the higher frequencies; however, with the high T_{IF} used, tuning for minimum F_R will tend to reduce L_s at the cost of higher T_M. Several of the points at the lower frequencies provide further suggestion of parametric effects.

Also included in Table V is a sample of other published room-temperature mixer results in the 30–70-GHz frequency range. In some cases, insufficient data was available to specify mixer performance completely. Not included in this sample are results for broad-band mixers [38], [40], in which instantaneous bandwidths of 20–30 GHz are achieved at the expense of increased conversion loss.

VI. SUMMARY AND CONCLUSIONS

This paper describes the design of the two-diode subharmonically pumped stripline mixer, the advantages of this circuit in comparison with conventional mixers, and its performance over the 47–110-GHz frequency range. The notch-front diode, which has ohmic contacts on the chip faces adjacent to the face containing the diode junctions, is described along with an outline of the processing steps for making this chip and mounting it on a strip transmission line circuit. The geometry and size of the notch-front diode results in a lower series resistance than for a conventional millimeter-wave diode, and can bring to stripline circuits the benefits of low parasitic reactance found in the waveguide wafer diode mount.

The performance of the two-diode subharmonically pumped mixer with notch-front diodes was found to be comparable to that of the best fundamental mixers. Even with commercial beam-lead diodes, the performance of the two-diode subharmonically pumped mixer compares favorably with other mixers over much of the millimeter-wave region.

Finally, evidence was seen in these results of parametric effects producing a reduction in mixer noise temperature to below the generally recognized limit for pumped resistive mixers.

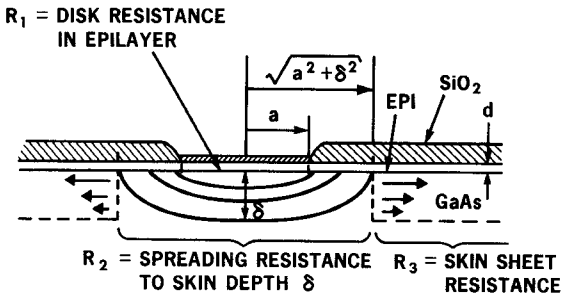

Fig. 17. Sources of RF series resistance in a millimeter-wave diode.

Appendix A

Sources of Series Resistance

The contributions to the diode millimeter-wave series resistance are shown in Fig. 17. The disk resistance in the epilayer is given by

$$R_1 = \frac{\rho_{epi} d}{\pi a^2} \tag{A-1}$$

where ρ_{epi} is the epilayer resistivity, d is the epilayer thickness, and a is the junction radius. The spreading resistance from the disk to one skin depth δ in the substrate is [40]

$$R_2 = \frac{\rho_s}{2\pi a} \arctan \frac{\delta}{a} \tag{A-2}$$

where ρ_s is the substrate resistivity.

Calculation of the skin sheet resistance is simplified if a circular geometry is assumed with the junction at the center of a chip of circular cross section with radius b and height h. The skin sheet resistance for a conventional chip is then [15]

$$R_3 = \frac{\rho_s}{2\pi\delta}\left[\ln \frac{b}{\sqrt{a^2+\delta^2}} + \frac{h}{b}\right]. \tag{A-3}$$

The sides of mechanically separated chips are not smooth, so the second term in (A-3) underestimates the actual sheet resistance of the sides. The sides of a notch-front diode are plated with gold and the second term in (A-3) is negligible.

Some typical values for the millimeter-wave diodes parameters are

$$\rho_{epi} = 8 \times 10^{-3}\ \Omega \cdot \text{cm}$$
$$\rho_s = 1 \times 10^{-3}\ \Omega \cdot \text{cm}$$
$$a = 1\ \mu\text{m}$$
$$d = 0.1\ \mu\text{m}$$
$$h = 100\ \mu\text{m}$$
$$\delta(100\ \text{GHz}) = 5\ \mu\text{m}$$
$$b = \begin{cases} 50\ \mu\text{m}, & \text{notch-front diode} \\ 125\ \mu\text{m}, & \text{conventional chip.} \end{cases}$$

The contributions to the series resistance are then

$$R_1 = 2.5\ \Omega$$
$$R_2 = 2.2\ \Omega$$
$$R_3 = \begin{cases} 0.7\ \Omega, & \text{notch front diode} \\ 1.2\ \Omega, & \text{conventional chip.} \end{cases}$$

The size and geometry of the notch-front diode lead to a 40-percent reduction in the sheet resistance term. This reduction is about 10 percent of the total series resistance, which is dominated by the resistance at the junction. The junction diameter and epilayer thickness vary with processing parameters, however, and the resulting variations in R_1 are larger than the calculated reduction in R_3 for the notch-front diode, so that experimental verification of this reduction would be difficult.

Appendix B

Error Estimates

Consider a quantity y which is a function of variables x_i so that $y = y(x_i)$. Then the variance of y is given by

$$\sigma_y^2 = \sum_i \left(\frac{\partial y}{\partial x_i}\right)^2 \sigma_{x_i}^2 \tag{B-1}$$

where $\sigma_{x_i}^2$ is the variance of x_i and it is assumed that the x_i's are uncorrelated. Equation (B-1) will be applied to the various quantities which describe mixer performance. All quantities used below are defined in the main text except $R = L_s/L_i$. In the examples, noise temperatures are rounded to 10 K and conversion losses to 0.1 dB.

Single-Sideband Receiver Noise Temperature:

$$T_R = \frac{T_H - YT_C}{Y-1}(1+R) \tag{B-2}$$

$$\sigma_{T_R}^2 = \left(\frac{1+R}{Y-1}\right)^2\left[\sigma_{T_H}^2 + Y^2\sigma_{T_C}^2 + \left(T_C + \frac{T_R}{1+R}\right)^2\sigma_Y^2\right] + \left(\frac{T_R}{1+R}\right)^2\sigma_R^2. \tag{B-3}$$

Mixer Noise Temperature:

$$T_M = T_R - L_s T_{IF} \tag{B-4}$$

$$\sigma_{T_M}^2 = \sigma_{T_R}^2 + T_{IF}^2\sigma_{L_s}^2 + L_s^2\delta_{T_{IF}}^2. \tag{B-5}$$

Conversion Loss Measured from Noise Power:

$$L_s = \frac{(T_H - T_C)(1+R)}{(Y_H - Y_C)(T_H + T_{IF})} \tag{B-6}$$

$$\sigma_{L_s}^2 = \left[\frac{L_s}{T_H - T_C}\right]^2\sigma_{T_C}^2 + \left[\frac{L_s}{1+R}\right]^2\sigma_R^2 + \left[\frac{L_s}{Y_H - Y_C}\right]^2\left(\sigma_{Y_H}^2 + \sigma_{Y_C}^2\right) + \left[\frac{L_s}{T_H + T_{IF}}\right]^2\sigma_{T_{IF}}^2 + \left[\frac{L_s(T_C + T_{IF})}{(T_H + T_{IF})(T_H - T_C)}\right]^2\sigma_{T_H}^2. \tag{B-7}$$

Examples:

Example I. Mixer 113, $f=98$ GHz

$$Y=1.145\pm.004 \qquad T_H=299\pm2\ \text{K}$$
$$L_s=7.4\pm0.5\ \text{dB} \qquad T_C=77\pm3\ \text{K}$$
$$R=2.9\pm0.3\ \text{dB} \qquad T_{\text{IF}}=330\pm5\ \text{K}$$
$$1+R=1.51\pm0.04 \qquad T_R(\text{SSB})=2204\ \text{K}$$
$$\sigma_{T_R}=100\ \text{K((B-3))}$$
$$\sigma_{T_M}=250\ \text{K((B-5))}.$$

Example II. Mixer 225 $f=94$ GHz

$$Y=1.306\pm.004 \qquad T_H=229\pm2\ \text{K}$$
$$Y_H=0.961\pm.004 \qquad T_C=77\pm3\ \text{K}$$
$$Y_C=0.735\pm.004 \qquad T_{\text{IF}}=108\pm5\ \text{K}$$
$$R=0.7\pm0.3\ \text{dB} \qquad T_R(\text{SSB})=1199\ \text{K}$$
$$1+R=1.85\pm0.06 \qquad L_s=6.5\ \text{dB}$$
$$\sigma_{T_R}=50\ \text{K((B-3))}$$
$$\sigma_{L_s}=0.2\ \text{dB((B-7))}$$
$$\sigma_{T_M}=60\ \text{K((B-5))}. \qquad \text{(B-8)}$$

ACKNOWLEDGMENT

The authors acknowledge the assistance of A. C. Chipaloski in measuring receiver performance and of A. A. Olenginski in processing notch-front diodes and useful discussions with E. T. Harkless, W. W. Snell, Jr., and R. F. Trambarulo. R. A. Linke suggested the form of the noise relationships in Figs. 9 and 10 and contributed to our understanding of (4)–(6). The authors also wish to thank A. R. Kerr for providing a preprint of a paper discussing the mixer noise theory expressed in (9).

REFERENCES

[1] M. V. Schneider and W. W. Snell, Jr., "Harmonically pumped stripline down-converter," *IEEE Trans. Microwave Theory Tech.*, vol. MTT-23, pp. 271–275, Mar. 1975.
[2] M. Cohn, J. E. Degenford, and B. A. Newman, "Harmonic mixing with an antiparallel diode pair," *IEEE Trans. Microwave Theory Tech.*, vol. MTT-23, pp. 667–673, Aug. 1975.
[3] P. S. Henry, B. S. Glance, and M. V. Schneider, "Local-oscillator noise cancellation in the subharmonically pumped down-converter," *IEEE Trans. Microwave Theory Tech.*, vol. MTT-24, pp. 254–257, May 1976.
[4] T. F. McMaster, M. V. Schneider, and W. W. Snell, Jr., "Millimeter-wave receivers with subharmonic pump," *IEEE Trans. Microwave Theory Tech.*, vol. MTT-24, pp. 948–952, Dec. 1976.
[5] R. J. Bauer, M. Cohn, J. M. Cotton, Jr., and R. F. Packard, "Millimeter wave semiconductor diode detectors, mixers, and frequency multipliers," *Proc. IEEE*, vol. 54, pp. 595–605, Apr. 1966.
[6] P. F. Goldsmith and R. L. Plambeck, "A 230-GHz radiometer system employing a second-harmonic mixer," *IEEE Trans. Microwave Theory Tech.*, vol. MTT-24, pp. 859–861, Nov. 1976.
[7] M. V. Schneider and E. R. Carlson, "Notch-front diodes for millimeter-wave integrated circuits," *Electron. Lett.*, vol. 13, pp. 745–747, Nov. 1977.
[8] T. F. McMaster, E. R. Carlson, and M. V. Schneider, "Subharmonically pumped millimeter-wave mixers built with notch-front and beam-lead diodes," presented at 1977 *IEEE-MTT-S Int. Microwave Symp. Digest*, San Diego, CA, June 21–23, 1977, pp. 389–392.
[9] AEI Semiconductors, Ltd., type DC 1308.
[10] C. A. Burrus, "Pulse electroplating of high-resistance materials, poorly contacted devices and extremely small areas," *J. Electrochem. Soc.*, vol. 118, pp. 833–834, May 1971.
[11] M. V. Schneider, R. A. Linke, and A. Y. Cho, "Low-noise millimeter-wave mixer diodes prepared by molecular beam epitaxy (MBE)," *Appl. Phys. Lett.*, vol. 31, pp. 219–221, Aug. 1, 1977.
[12] D. T. Young and J. C. Irvin, "Millimeter-frequency conversion using Au-n-type GaAs Schottky barrier epitaxial diodes with a novel contacting technique," *Proc. IEEE*, vol. 53, pp. 2130–2131, Dec. 1965.
[13] D. N. Held and A. R. Kerr, "Conversion loss and noise of microwave and millimeter-wave mixers: part 2—experiment," *IEEE Trans. Microwave Theory Tech.*, vol. MTT-26, pp. 55–61, Feb. 1978.
[14] J. A. Calviello, J. L. Wallace, and P. R. Bie, "High performance GaAs quasi-planar varactors for millimeter waves," *IEEE Trans. Electron. Devices*, vol. ED-21, pp. 624–630, Oct. 1974.
[15] Indium Corporation of America, Indalloy No. 2.
[16] Indium Corporation of America, Indalloy No. 8.
[17] F. Rosebury, *Handbook of Electron Tube and Vacuum Techniques*. Reading, MA: Addison-Wesley, 1965, p. 20.
[18] W. W. Mumford and E. H. Scheibe, *Noise Performance Factors in Communications Systems*. Dedham, MA: Horizon House—Microwave, 1968, pp. 20–21.
[19] [18, pp. 25–32].
[20] [18, p. 42].
[21] AILTECH Type 70 Hot-Cold Standard Noise Generator.
[22] Hewlett-Packard Models 435A and 8481A.
[23] Hitachi Model E-3904.
[24] [18, pp. 61–64].
[25] A. R. Kerr, "Low-noise room-temperature and cryogenic mixers for 80–120 GHz," *IEEE Trans. Microwave Theory Tech.*, vol. MTT-23, pp. 781–787, Oct. 1975.
[26] W. J. Wilson, "The Aerospace low-noise millimeter-wave spectral line receiver," *IEEE Trans. Microwave Theory Tech.*, vol. MTT-25, pp. 332–335, Apr. 1977.
[27] P. Zimmermann and R. W. Haas, "A broadband low noise mixer for 106–116 GHz," *Nachrichtentech. Z.*, vol. 30, pp. 721–722, Sept. 1977.
[28] R. A. Linke and M. V. Schneider in *Workshop on Mixers at Millimeter Wavelengths*, Max-Planck-Institut für Radioastronomie, Bonn, Apr. 26–28, 1977.
[29] C. Dragone, "Analysis of thermal and shot noise in pumped resistive diodes," *B.S.T.J.*, vol. 47, pp. 1883–1902, Nov. 1968.
[30] A. A. M. Saleh, *Theory of Resistive Mixers*, Cambridge, MA: M.I.T. Press, 1971, p. 170.
[31] D. N. Held and A. R. Kerr, "Conversion loss and noise of microwave and millimeter-wave mixers: Part 1—theory," *IEEE Trans. Microwave Theory Tech.*, vol. MTT-26, pp. 49–55, Feb. 1978.
[32] Signalite Model TN-164.
[33] S. Weinreb and A. R. Kerr, "Cryogenic cooling of mixers for millimeter and centimeter wavelengths," *IEEE J. Solid-State Circuits*, vol. SC-8, pp. 58–63, Feb. 1973.
[34] J. A. Calviello and J. L. Wallace, "Performance and reliability of an improved high temperature GaAs Schottky junction and native-oxide passivation," *IEEE Trans. Electron Devices*, vol. ED-24, pp. 698–704, June 1977.
[35] J. J. Whelehan, "Low-noise millimeter-wave receivers," *IEEE Trans. Microwave Theory Tech.*, vol. MTT-25, pp. 268–280, Apr. 1977.
[36] M. Akaike, N. Kanmuri, H. Kato, and K. Hiyama, "Millimeter-wave solid-state circuits," *Rev. Elect. Commun. Laboratories*, vol. 23, pp. 904–918, July–August 1975.
[37] P. J. Meier, "Low-noise mixer in oversized microstrip for 5-mm band," *IEEE Trans. Microwave Theory Tech.*, vol. MTT-22, pp. 450–451, Apr. 1974.
[38] A. Hislop and R. T. Kihm, "A broad-band 40-60-GHz balanced mixer," *IEEE Trans. Microwave Theory Tech.*, vol. MTT-24, pp. 63–64, Jan. 1976.
[39] L. T. Yuan, G. M. Yamaguchi, and J. E. Raue, "Design, implementation, and performance analysis of a broad-band V-band network analyzer," *IEEE Trans. Microwave Theory Tech.*, vol. MTT-24, pp. 981–987, Dec. 1976.
[40] L. T. Yuan, "Low noise octave bandwidth waveguide mixer," 1977 *IEEE MTT-S Int. Microwave Symp. Dig.* (San Diego, CA), June 21–23, 1977, pp. 480–482.
[41] R. Holm, *Electric Contacts*. New York: Springer-Verlag, 1967, pp. 15–16.